

**DESIGN AND DEVELOPMENT OF BAND
PASS FILTER MICROSTRIP CASCADE TRISECTION
WITH OPEN STUB AND DEFECTED GROUND
STRUCTURE (DGS) IN 1800 MHz FREQUENCY**

ENJANG AKHMAD JUANDA*, TOMMI HARIYADI, MUKHIDIN,
USUP, REGITA NURMALITA YUNIAR

Departemen Pendidikan Teknik Elektro, Universitas Pendidikan Indonesia,
Jalan Dr. Setiabudhi No. 229, 40154, Bandung, Indonesia

*Corresponding Author: juanda@upi.edu

Abstract

The rapid development of technology has resulted in the growth of the number of mobile communication service users. One technology that is currently being developed is Long Term Evolution (LTE), which allows sending data at higher speeds. To support LTE technology, various components and devices are required. One device needed is a band pass filter (BPF). In this research, we designed BPF micro strip cascade trisection at 1,800 MHz frequency for 4G LTE applications. Simulation and optimization are carried out using CST Studio suite 2012. The material used as a substrate material is Rogers RT5880, which has a dielectric constant of 2.2 and a thickness of 1.6 mm. This study demonstrated that the designed BPF has a 75 MHz bandwidth at a frequency of 1,805-1,880 MHz with a return loss of -10.26 dB, insertion loss of -1.29 dB and VSWR of 1.28.

Keywords: 4GLTE, Band-pass filter, Cascade trisection, DGS, Microstrip, Open stub.

1. Introduction

The development of mobile communication technology is developing and increasing rapidly. As the number of mobile communication service users is increasing, the need for a variety of communication services and the development of technology that supports high-speed data transmission and higher traffic is increasing [1]. One technology that is currently developing to support services with large amounts of high-speed data is Long Term Evolution (LTE) [2]. LTE has many advantages including downlink data transmission of more than 100 Mbps with low latency, and the use of very efficient spectrum. LTE is a new standard to increase the capacity and speed of the current network. LTE is often referred to as 4G (fourth generation) [3]. To support LTE technology, various devices are needed. One device that plays an important role in the application of mobile communication technology is a filter. Because of the LTE bandwidth is wide, a band-pass filter (BPF) is needed to prevent interference before the signal reaches the antenna [4, 5]. Filters are indispensable devices in many wireless systems and applications, including wireless broadband, mobile, satellite communications, radar, navigation, and other sensing systems [6]. The number of orders is an important parameter commonly used in designing the filter. Active or passive filter circuit employs higher-order filter circuits to ensure that both corner frequency noises are completely removed. Therefore, it will be decreasing the interference signal [7].

Cascade trisection is a development of trisection filter, which is a cross-coupled filter. Unlike the hairpin method that has zero transmission results, with the cascade trisection method, the resulting transmission zero has a frequency response with step sides on both sides of the passband [8]. The Defected Ground Structure (DGS) used in the design is used to improve the return loss value of the BPF [9]. DGS is installed on the ground (under the feed tap of BPF), which is located obtained from the results of optimization [10]. Open Stub is a resonator component that is added to an existing resonator, however, the size is not the same as the cascade trisection resonator.

Based on studies by Sarkar et al. [11], the longer the size of the open stub, the narrower the bandwidth produced. Some parameters that are considered in the filter are return loss, insertion loss, VSWR, and impedance [12]. Most of the BPF designs are using microstrip structure. In the microstrip design structure, the higher frequency operating is the smaller the circuit [13]. Numerous studies about band-pass filter have been carried out previously using some structures. That studies such as band-pass filters on U-shaped resonators with three identical resonators [14], triple U-shaped defected ground structure (DGS) [15], band-pass filter using open-circuited stub [11], a combination of DGS's and open-ended slot [16], and the like. Letavin [14] mentioned that the return loss and insertion loss have good value, however, the insertion loss value still high enough. Avinash and Rao [15] proposed that filter design using U shaped DGS, in which, has the benefit of low insertion loss and high selectivity, however, this design used for ultra-wideband (UWB) application and not suitable for LTE application. Ghosh and Mondal [16] stated that the return loss and insertion loss value are good, however, the band-pass response still not sharp and stable. In this study, we designed BPF using open stub and DGS. The expected BPF specification can work at a frequency of 1800 MHz with a return loss below -10 dB, insertion loss of around -1 dB and $1 < \text{VSWR} < 2$.

2. Research Methods

This research is a type of experimental research, which includes simulation, optimization, and fabrication. In the initial stage, a literature study is carried out, then a specification is determined and followed by a design and manufacturing stage consisting of simulations and optimizations with CST Studio Suite 2012 software. This process is carried out until parameters are in accordance with the specified specifications.

The initial stages of designing this BPF are determining the desired characteristics or parameters. The type of substrate used in this study is Rogers RT5880, which has a thickness (h) of 1.6 mm and a relative dielectric constant (ϵ_r) of 2.2 and a Dielectric Loss Tangent (δ) of 0.0009.

Table 1 shows the desired specifications of the designed BPF. The filter we designed has six filter's order. The increasing of the number of filter order has the effect of increasing the sharpness of filter response. The specifications of the filter designed in this study including of operating frequency, half power bandwidth, center frequency, Fractional bandwidth, insertion loss, return loss, impedance, VSWR, filter order, and frequency response.

The design of the Cascade Trisection BPF construction consists of six resonators. The first step is calculation of the resonance frequencies of the six resonators. Then determine the dielectric constant, the length of the resonator, the width of the supply channel, the length of the open stub, and the dimensions of the DGS size. This calculation is done in order to get the desired frequency response. The following outlines the calculations of some parts of the micro strip filter.

Table 1. Specifications of BPF designed.

No.	Specification	Value
1.	Operating frequency	1,805-1,880 MHz
2.	Bandwidth -3 dB	75 MHz
3.	Center frequency	1,843 MHz
4.	FBW (fractional BW)	0.03
5.	Insertion loss	< -2 dB
6.	Return loss	< -10 dB
7.	Matching impedance	50 ohm
8.	VSWR	1 < VSWR < 2
9.	Filter order	6
10.	Frequency response	Chebyshev

2.1. Determine the resonance frequencies

In the Cascade Trisection BPF design, the value of this resonant frequency can be obtained by Eq. (1) [10].

$$f_{0n} = f_0 \sqrt{1 - \frac{B_n}{g_n / FBW + B_n / 2}} \quad (1)$$

where f_{0n} is the n^{th} resonance frequency, f_0 is the middle frequency, B_n is the bandwidth at the n^{th} frequency. From Eq. (1), we get $f_{01} = 1,820$ MHz, $f_{02} = 1,825.80$ MHz, $f_{03} = 1,841.72$ MHz, $f_{04} = 1,823.83$ MHz, and $f_{05} = 1,842.00$ MHz.

After that, the design is continued by determining the width of the supply channel as a place to put the connector using Eqs. (2) and (3) [10]. This line uses 50Ω channel impedance to obtain maximum power transfer. The width and shape of the supply channel can be seen in Fig. 1. In Eq. (2), A is the constant that needed to calculate the resonator channel width (W) in mm, with d is the distance between each resonator in mm, and Z_0 is the characteristic impedance of the transmission line.

$$A = \frac{Z_0}{60} \sqrt{\frac{\epsilon_r + 1}{2}} + \frac{\epsilon_r - 1}{\epsilon_r + 1} \left(0.23 + \frac{0.11}{\epsilon_r} \right) \tag{2}$$

Then, the value of $A = 1.159$

$$\frac{W}{d} = \frac{8e^A}{e^{2A} - 2} \tag{3}$$

$$\frac{W}{d} = 3.126$$

Because $W / d > 2$, the resonator channel width is:

$$W = W/d \times h = 3.13 \times 1.6 = 5.008 \text{ mm}$$

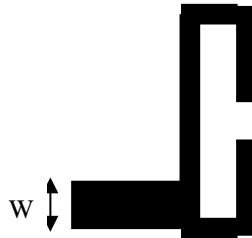


Fig. 1. Width of the feeding channel.

2.2. Determine the resonator length

Before determining the length of each resonator, first we determine the value of the effective dielectric constant (ϵ_{eff}). The effective dielectric constant value will vary for each channel, this depends on the width of the channel used. Designing this filter using the channel width (W) = 1 mm because the bandwidth at the frequency used is quite wide. Effective Dielectric Constants (ϵ_{eff}) can be found using Eq. (4):

$$\epsilon_{eff} = \frac{\epsilon_r + 1}{2} + \frac{\epsilon_r - 1}{2} \sqrt{\frac{1}{1 + 12 \left(\frac{h}{W} \right)^2}} \tag{4}$$

Therefore, we obtained $\epsilon_{eff} = 1.87$.

2.3. Designing the distance between resonators

In the previous equation, the value $f_{0l} = f_{0m}$ that has been obtained is entered into Eq. (5) as the cut-off frequency value to get the wavelength value. After that, the wavelength value of each resonator is entered in Eq. (6) to obtain the length of each resonator channel.

$$\lambda_{gn} = \frac{c}{f_{cutoff} n^{th} \sqrt{\epsilon_{eff}}} \tag{5}$$

With,

$$l_{an} = \frac{\lambda_{gn}}{2} \tag{6}$$

Using Eq. (5), wavelengths are obtained from each resonator on the BPF. While the resonator length value is obtained from Eq. (6). From Eq. (5), c is the light speed in m/s and $f_{cutoffn^{th}}$ is the n^{th} cut off frequency. The results obtained are shown in Table 2. The λ_{gn} is the n^{th} ground wavelength and l_a is the length of the resonator.

Figure 2 shows the design of each designed resonator. The length of the gap in each resonator is a half wavelength. In all resonators except 2nd, resonator have bands in every corner.

Table 2. Length of each resonator.

n	f_n (MHz)	λ_{gn} (mm)	l_a (mm)
1	1,821	111.6	55.80
2	1,810	119	59.50
3	1,807	119	59.50
4	1,804	120.2	60.14
5	1,793	119.09	59.54
6	1,821	111.6	55.80

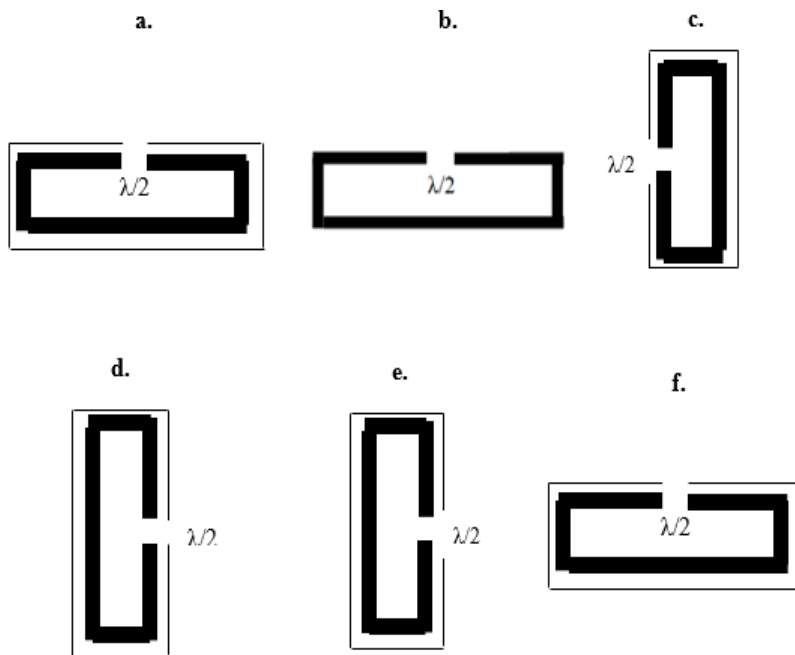


Fig. 2. The geometry of each resonator used in this study:
 a) 1st resonator length, b) 2nd resonator length, c) 3rd resonator length,
 d) 4th resonator length e) 5th resonator length, f) 6th resonator length.

2.4. Open stub design

The design of open stub aims to narrow the bandwidth according to the expected specifications. An open stub is a resonator component that is added to an existing resonator, however, the size of the open stub resonator is not the same as the cascade trisection resonator. The longer size of the open stub, the narrower the bandwidth that is generated. The expected bandwidth is carried out by optimize the length of open stub five times from the length of 0.1 to 0.5. Table 3 shows the results of the optimization of the open stub on the second and fifth resonators.

Table 3. Optimization results of open stub's length.

Length (mm)	f_1 (MHz)	f_2 (MHz)	Middle frequency (MHz)	Bandwidth (MHz)
0.5	1,821	1,870	1,839	49
0.4	1,810	1,875	1,841	65
0.3	1,807	1,880	1,845	73
0.2	1,804	1,885	1,851	81
0.1	1,793	1,890	1,860	97

2.5. DGS design

DGS is used to improve the return loss value of BPF. The DGS is mounted on the ground (under the feed/tap of the BPF) whose location is obtained based on optimization. Figure 3 shows the geometry and design parameters of the DGS.

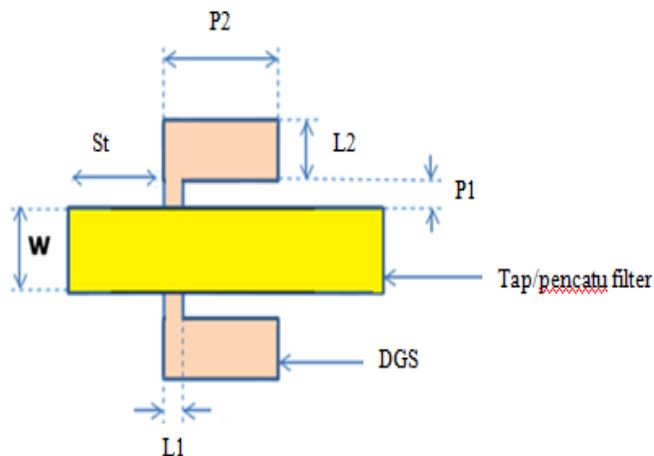


Fig. 3. Dimension of defected ground structure.

2.6. Final simulation results of the cascade trisection BPF microstrip using open stub and DGS

After calculating the dimensions of the filter, then continue with optimization on the dimensions of the BPF. Figure 4 shows the dimensions of the designed BPF in accordance with the expected specifications.

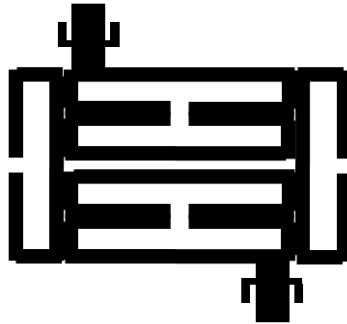


Fig. 4. The final dimension of the BPF cascade trisection.

3. Results and Discussion Simulation results

After optimize the L_r resonator length, resonator distance (S), tap width (W), open stub length (L_{os}) and DGS size, BPF simulation results are obtained according to specifications. The S_{21} simulation results from the designed BPF are shown in Fig. 5, while the S_{11} simulation results are shown in Fig. 6. Figure 5 shows the comparison of the insertion loss to frequency, besides Fig. 6 shows the comparison of return loss to frequency. Return loss and insertion loss is the most important parameters of all the devices, including filter. Figure 5 shows the comparison chart of insertion loss in dB to a frequency in GHz. It can be observed that the value of insertion loss at the frequency of 1,852 MHz is -1.29 dB and the operating frequency of BPF is 1,805-1,880 MHz with a bandwidth of 75 MHz.

Figure 6 shows the results of S_{11} simulation to frequency. As we can see that the value of return loss at the frequency of 1,852 MHz is -10.26 dB. The value of return loss in frequency 1,880.4 MHz is -16.795 dB. The highest value of return loss is about -25 dB in frequency 1,834 MHz. To make the simulation results in the form of a band-pass can be done by changing the location of the Tap/feeder without changing the size of the tap/feeder calculation results. The use of open stub on the BPF resonator is able to narrow the bandwidth. Changing the resonator length can increase the value of return loss.

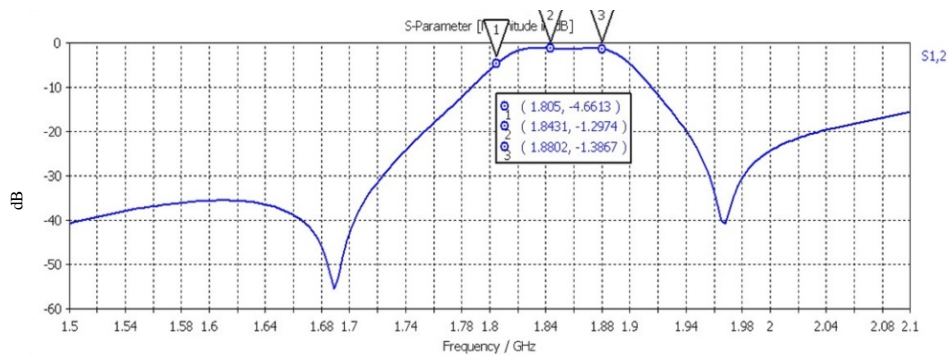


Fig. 5. Insertion loss (S_{21}) chart from simulation.

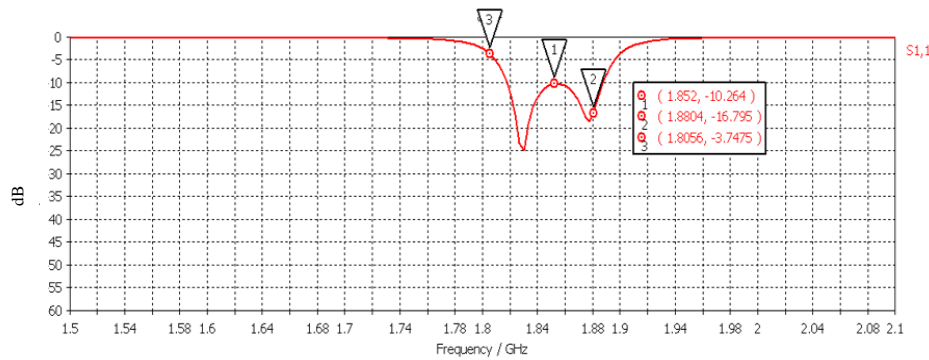


Fig. 6. Return loss (S_{11}) chart from simulation.

3.2. Fabrication results and test equipment

The design of the cascade trisection microstrip BPF with open stub and DGS was simulated with CST 2012 software, which was then fabricated and measured using a Vector Network Analyser (VNA). The cascade trisection BPF fabrication results are shown in Fig. 7. The final dimensions of the fabricated cascade trisection BPF are 60 mm \times 45 mm. Measurements were taken at BPF using the Advantest R3770 two-port Network Analyser. BPF parameters that can be measured in this measurement include measurement of return loss (S_{11}), insertion loss (S_{21}) and VSWR measurement. Based on the results obtained, the measurement results are close to the simulation results. For more details regarding the comparison of measurement results with simulation results for the values of S_{11} and S_{21} can be seen in Figs. 8 and 9. The return loss and the insertion loss measured in dB unit and comparison to an operating frequency in GHz. Return loss describes the performance of the device, in which the value must be less than -10 dB. Meanwhile, for a two-port device, the ideal insertion loss value is close to 0 dB.

Figure 8 shows that the reflection parameter (S_{11}) of two different conditions, namely the simulation results and measurement results. S_{11} responses from the simulation process showed better results compared to measurement results. The bandwidth of the BPF measurement results is wider than the simulation results. It can be seen from Fig. 9 that the transmission parameter (S_{21}) of the simulation results has difference with the measurement results, where the expected response is slightly shifted. This difference can occur due to differences in conditions between simulation and measurement and the effect of connecting the device with the SMA connector used.

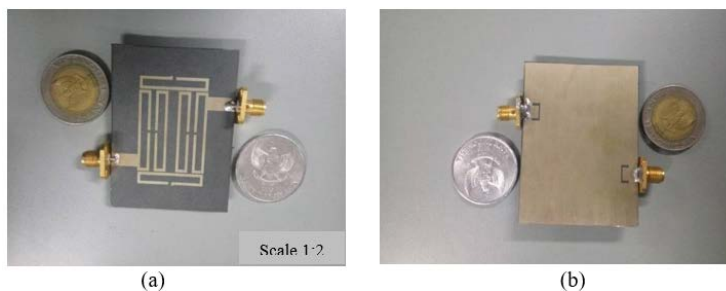


Fig. 7. Design of equipment: (a) Front-end and (b) Rear-end fabrication.

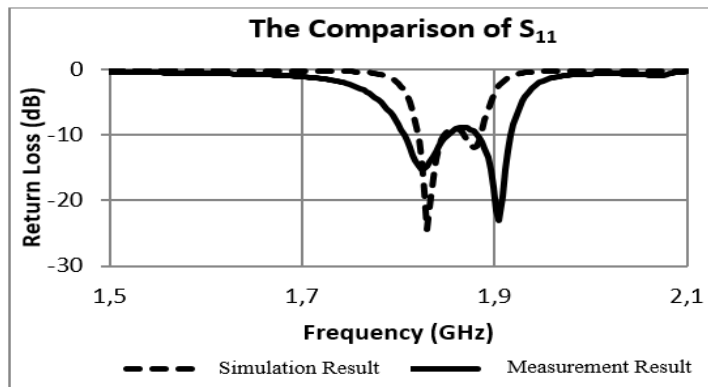


Fig. 8. S_{11} comparison chart of measurement results and simulation results.

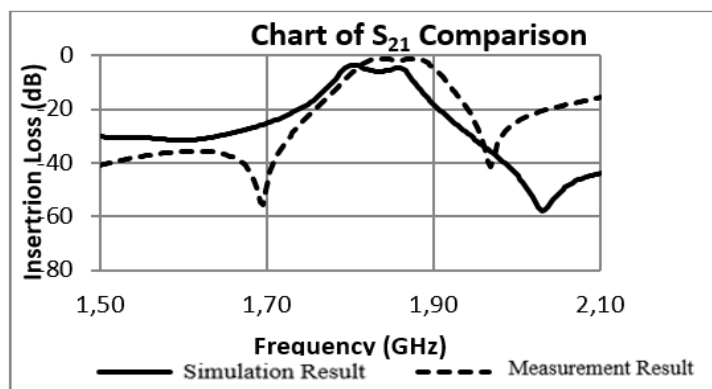


Fig. 9. The Comparison of S_{21} between measurement and simulation.

4. Conclusion

In this paper, a band-pass filter micro strip cascade trisection has been designed and manufactured using Rogers RT5880 with the 1.6 mm and 2.2 of the thickness and dielectric constant respectively. It has a frequency range from 1,805 to 1,880 MHz with a return loss less than -10 dB, insertion loss about -1.29 dB and VSWR of 1.28. Based on the comparison that has been made between the simulations results with the measurement results, the differences that arise can be caused by several factors. In this study, the use of DGS has no significant effect in increasing the value of return loss, however, it does affect the increase in the cut-off frequency thereon.

References

1. Gonzalez, G. (1997). *Microwave transistor amplifiers: Analysis and design* (2nd ed.). Upper Saddle, New Jersey, United States of America: Prentice Hall.
2. Karthaus, U.; Sukumaran, D.; Tontisirin, S.; Ahles, S.; Elmaghraby, A.; Schmidt, L.; and Wagner, H. (2012). Fully integrated 39 dBm, 3-stage Doherty

- PA MMIC in a low-voltage GaAs HBT technology. *IEEE Microwave and Wireless Components Letters*, 22(2), 94-96.
3. Taneja, S.; Gautam, J.; and Sharma, J. (2016). Design and performance analysis of 2.5 GHz microstrip bandpass filter for LTE. *Proceedings of the Second International Conference on Computational Intelligence & Communication Technology (CICT)*. Ghaziabad, India, 549-553.
 4. Maas, S.A. (2003). *Nonlinear microwave and RF circuits* (2nd ed.). Norwood, Massachusetts, United State of America: Artech House, Inc.
 5. Li, Y.C.; Wu, K.C.; and Xue, Q. (2013). Power amplifier integrated with bandpass filter for long term evolution application. *IEEE Microwave and Wireless Components Letters*, 23(8), 424-426.
 6. Liu, X.Y.; Zheng, H.X.; Li, Y.J.; and Feng, L.Y. (2015). Compact wide-band bandpass filter using dual mode capacitance loaded meander square ring resonator with open stubs. *Proceedings of the 4th International Conference on Computer Science and Network Technology (ICCSNT)*. Harbin, China, 40(1), 963-966.
 7. Jamaluddin, F.N.; Ahmad, S.A.; Hassan, W.Z.W.; and Noor, S.B.M. (2016). Filtering corner frequency using undecimated wavelet transform for surface EMG. *Journal of Engineering Science and Technology (JESTEC)*, Special Issue on WRICET2016, December (2018), 61-70.
 8. Wibisono, G.; Firmansyah, T.; and Syafraditya, T. (2016). Design of triple-band bandpass filter using cascade tri-section stepped impedance resonators. *Journal of ICT Research and Applications*, 10(1), 43-56.
 9. Hariyadi, T.; Huda, Y.T.; and Mulyanti, B. (2016). A small ultra-wideband unidirectional microstrip antenna for through-wall radar application. *Journal of Telecommunication, Electronic and Computer Engineering (JTEC)*, 8(1), 25-28.
 10. Leong, C.C.; Ting, S.W.; and Tam, K.W. (2008). Multi-spurious suppression for microstrip dual-mode bandpass filter using triple U-shaped defected ground structure. *Proceedings of the IEEE Asia Pacific Conference on Circuits and Systems (APCCAS)*. Macao, China, 90-92.
 11. Sarkar, P.; Ghatak, R.; Pal, M.; and Poddar, D.R. (2012). Compact UWB bandpass filter with dual notch bands using open circuited stubs. *IEEE Microwave and Wireless Components Letters*, 22(9), 453-455.
 12. Pozar, D.M. (2012). *Microwave Engineering* (4th ed.). Hoboken, New Jersey, United States of America: John Wiley & Sons, Inc.
 13. Fauzi, A.; and Rizman, Z.I. (2016). Design and fabrication of 12 GHz microstrip directional coupler for RF/microwave application. *Journal of Engineering Science and Technology (JESTEC)*, 11(3), 431-442.
 14. Letavin, D.A. (2018). Band-pass filters on u-shaped resonators. *Proceedings of the 19th International Conference of Young Specialists on Micro/Nanotechnologies and Electron Devices (EDM)*. Erlagol, Russia, 6403-6408.
 15. Avinash, K.G.; and Rao, I.S. (2015). Design of microstrip wideband bandpass filter using U shaped defected ground structure. *Proceedings of the International Conference on Microwave, Optical and Communication Engineering (ICMOCE)*. Bhubaneswar, India, 103-105.
 16. Ghosh, A.; and Mondal, P. (2018). Bandpass filter using a combination of DGS's and open ended slot. *Proceedings of the 2nd International Conference on Trends in Electronics and Informatics (ICOEI)*. Tirunelveli, India, 392-396.